



Published in final edited form as:

*Chem Commun (Camb)*. 2014 December 7; 50(94): 14835–14838. doi:10.1039/c4cc07027e.

## Oxidation-responsive Eu<sup>2+/3+</sup>-liposomal contrast agent for dual-mode magnetic resonance imaging†

Levi A. Ekanger<sup>a</sup>, Meser M. Ali<sup>b</sup>, and Matthew J. Allen<sup>a</sup>

Matthew J. Allen: mallen@chem.wayne.edu

<sup>a</sup>Department of Chemistry, Wayne State University, 5101 Cass Ave., Detroit, MI 48202, USA

<sup>b</sup>Department of Neurology, Henry Ford Hospital, 1 Ford Place, Detroit, MI 48202, USA

### Abstract

An oxidation-responsive contrast agent for magnetic resonance imaging was synthesized using Eu<sup>2+</sup> and liposomes. Positive contrast enhancement was observed with Eu<sup>2+</sup>, and chemical exchange saturation transfer was observed before and after oxidation of Eu<sup>2+</sup>. Orthogonal detection modes render the concentration of Eu inconsequential to molecular information provided through imaging.

The power of magnetic resonance imaging (MRI) resides in the ability to ascertain anatomical information at high resolution for clinical (1 mm isotropic) and preclinical (0.025 mm isotropic) applications.<sup>1</sup> Molecular information can also be obtained with MRI using responsive paramagnetic complexes (contrast agents) that alter water proton signal intensities in response to chemical events. Some contrast agents respond to changes in pH,<sup>2,3</sup> temperature,<sup>4</sup> metal ion concentration,<sup>5</sup> enzyme activity,<sup>6,7</sup> or partial pressure of oxygen,<sup>8</sup> the presence of free radicals,<sup>9</sup> antioxidants,<sup>10</sup> phosphate diesters,<sup>11</sup> singlet oxygen,<sup>12</sup> reduced glutathione and hydrogen peroxide,<sup>13</sup> or oxygen, dithionite, and cysteine.<sup>14</sup> Of particular interest are targets that cause changes in redox behavior because they are associated with cancer,<sup>15</sup> inflammation,<sup>16</sup> and cardiovascular diseases.<sup>17</sup> Accordingly, responsive contrast agents that target redox changes have the potential to greatly improve the diagnostic capabilities of MRI. However, a critical limitation of responsive contrast agents that hinders their use *in vivo* is that determination of molecular information requires knowledge of the concentration of contrast agent, which is exceedingly difficult to measure *in vivo*. Some systems have achieved concentration independence in contrast-enhanced MRI through ratiometric techniques (longitudinal vs. transverse relaxation rates),<sup>18</sup> ratiometric chemical exchange saturation transfer (CEST) techniques,<sup>2,12</sup> or the use of orthogonal detection modes with a multimodal agent;<sup>19</sup> however, to the best of our knowledge, no reported system demonstrates a concentration-independent response to general oxidizing events based on tunable oxidation potentials. An ideal metal ion for multimodal redox response is Eu<sup>2+</sup> because the Eu<sup>2+</sup> and Eu<sup>3+</sup> oxidation states orthogonally enhance  $T_1$ -weighted and CEST images, respectively, in MRI. Furthermore, Eu<sup>2+</sup> has a tunable

†Electronic supplementary information (ESI) available: Experimental procedures, preparation of hydration solution, preparation of liposomes, raw CEST data, Lorentzian function fitting, and dynamic light scattering data. See DOI: 10.1039/c4cc07027e

Correspondence to: Matthew J. Allen, mallen@chem.wayne.edu.

oxidation potential<sup>20</sup> and outperforms clinically approved  $T_1$ -shortening contrast agents at ultra-high magnetic field strengths.<sup>21</sup> To address the need for a concentration-independent, oxidation-responsive contrast agent, we hypothesized that encapsulating the  $\text{Eu}^{2+}$ -containing complex (4,7,13,16,21,24-hexaoxa-1,10-diazabicyclo[8.8.8]hexacosane europium(II),  $\text{Eu}(2.2.2)^{2+}$ , Fig. 1) in liposomes would produce an oxidation-responsive dual-mode contrast agent because it would enhance either  $T_1$ -weighted images or CEST images depending on the oxidation state of Eu.

Our design was based on the oxidation of  $\text{Eu}^{2+}$  to  $\text{Eu}^{3+}$  because these two oxidation states offer orthogonal modes of detection by MRI and the  $\text{Eu}^{2+/3+}$  oxidation state switch offers an ideal platform for oxidation-responsive contrast enhancement.<sup>8,22</sup> The use of this switch has awaited sufficient stabilization of  $\text{Eu}^{2+}$  that we recently demonstrated through modifications to  $\text{Eu}(2.2.2)^{2+}$  ligand structure.<sup>20</sup> Furthermore, changes to ligand structure made the corresponding oxidation potential of  $\text{Eu}^{2+}$  tunable over a physiologically relevant range.<sup>20</sup> Here, we report the encapsulation of  $\text{Eu}(2.2.2)^{2+}$  in liposomes and distinct oxidation-responsive, dual-mode imaging behavior. This system is expected to open the door for concentration-independent diagnostic imaging of redox-active disease states using the chemistry of Eu.

Our system used liposomes because their aqueous inner cavity can encapsulate water-soluble contrast agents to improve the sensitivity of CEST by increasing the ratio of chemically shifted water protons (associated with liposomes) to bulk water protons (not associated with liposomes).<sup>23</sup> Liposome composition was adapted from a report that used 1-palmitoyl-2-oleoyl-*sn*-glycero-3-phosphocholine and cholesterol,<sup>24</sup> and liposomes were characterized using dynamic light scattering. The average diameter measured before and after air exposure was  $110 \pm 7$  and  $106 \pm 6$  nm, respectively, where the diameter error is the standard error calculated from the average polydispersity index values. The average liposome polydispersity index value before and after air exposure was  $0.14 \pm 0.01$  and  $0.10 \pm 0.06$ , respectively, where the polydispersity index error is the standard error at the 95% confidence interval. These size distribution data indicate that average liposome size was not different before and after oxidation (Student's *t*-test) and, consequently, not affected by the intraliposomal formation of  $\text{Eu}^{3+}$ .

To evaluate the response of our liposomes, we encapsulated 45 mM  $\text{Eu}(2.2.2)^{2+}$  because of previous studies that loaded similar or higher concentrations of paramagnetic complexes into liposomes.<sup>4b,23</sup> After removing non-encapsulated  $\text{Eu}(2.2.2)^{2+}$  by spin filtering, we characterized suspensions of liposomes containing  $\text{Eu}(2.2.2)^{2+}$  before and after exposure to air. Molecular oxygen within air was chosen as a convenient source of oxidant to demonstrate a response corresponding to oxidation of  $\text{Eu}(2.2.2)^{2+}$ . This mechanism of response is most likely diffusion of oxygen into the buffer and across the liposome membrane. Once oxygen has crossed the membrane, it can oxidize  $\text{Eu}(2.2.2)^{2+}$  ( $T_1$  enhancing agent) to form  $\text{Eu}(2.2.2)^{3+}$  ( $T_1$  silent), and consequently, the response to oxidation can be detected by loss of  $T_1$  enhancement. Support for the oxygen diffusion mechanism was found by measuring the change in  $T_1$  as a function of air exposure for liposome suspensions containing  $\text{Eu}(2.2.2)^{2+}$ . Without stirring,  $\text{Eu}(2.2.2)^{2+}$  within liposomes required 7 h to oxidize in air. Upon stirring, however,  $\text{Eu}(2.2.2)^{2+}$  within

liposomes oxidized within 10 min of air exposure. Stirring the solution would facilitate an increased rate of oxygen diffusion, which would accelerate the rate of oxidation. To ensure complete oxidation of  $\text{Eu}(\text{2.2.2})^{2+}$  to form  $\text{Eu}(\text{2.2.2})^{3+}$  within the oxidized samples, liposomes were exposed to air for 24 h without stirring because of the small size of the sample tube prior to imaging. After air exposure we observed an 86% decrease in  $T_1$  (0.4 and 2.8 s for the same sample before and after air exposure, respectively, at 24 °C, 11.7 T, and 45 mM in Eu), which is a response similar to or greater than other reported contrast agents.<sup>25</sup> A rationale for the large change in  $T_1$  is that  $\text{Eu}^{2+}$  is isoelectronic with  $\text{Gd}^{3+}$ , but  $\text{Eu}^{3+}$  is diamagnetic in its ground state and is not expected to dramatically influence  $T_1$ . The observation of  $T_1$  changing upon air exposure is in good agreement with the  $T_1$ -shortening nature of  $\text{Eu}(\text{2.2.2})^{2+}$  (relaxivity was  $3.99 \text{ mM}^{-1} \text{ s}^{-1}$  outside of liposomes and  $0.2 \text{ mM}^{-1} \text{ s}^{-1}$  inside of liposomes at 20 °C and 11.7 T. The lower relaxivity is expected for  $T_1$ -shortening contrast agents encapsulated in spherical liposomes).<sup>21,26</sup> Furthermore, the change in  $T_1$  upon air exposure indicates that oxidation to form  $\text{Eu}(\text{2.2.2})^{3+}$  caused the observed lengthening of  $T_1$ .

To characterize the dual-mode behavior of Eu-containing liposomes, we investigated the CEST response before and after air exposure by measuring *in vitro* image intensities as a function of frequency offset of presaturation at 7 T. The intensity data (Fig. S1, ESI<sup>†</sup>) was modeled with a Lorentzian function using least squares fitting to reference the upfield signal to 0 ppm. Lorentzian fitting was used because the sample images were acquired simultaneously and the bulk water signals were not centered at 0 ppm. We chose to average the CEST spectra because it appeared that both the proximity to the bulk water signal and inhomogeneity in the magnetic field led to variability in the intensity measurements. The average CEST spectra (Fig. 2) revealed that liposomes before and after 24 h air exposure exhibited an exchangeable proton signal at 1.2 ppm relative to bulk water. Additionally, there was no significant difference between the CEST effect before and after oxidation of Eu (Fig. 2), which demonstrates that the CEST effect does not change after  $\text{Eu}(\text{2.2.2})^{2+}$  has oxidized to  $\text{Eu}(\text{2.2.2})^{3+}$ . Although this shift is small, it is possible to image such shifts *in vivo*:<sup>27,28</sup> *in vivo* CEST has been observed between bulk water and exchangeable protons of liposomes shifted by as little as 0.8 ppm.<sup>27</sup>

To investigate the cause of CEST effect before oxidation of Eu, we acquired CEST spectra for a series of samples including blank liposomes containing only phosphate-buffered saline, liposomes containing  $\text{Sr}(\text{2.2.2})^{2+}$  (28 mM Sr) as a diamagnetic analog, and liposomes containing four different concentrations of  $\text{Eu}(\text{2.2.2})^{2+}$  (13, 24, 40, and 45 mM Eu) (Fig. 2 and 3). CEST effect was observed for each sample as a broad signal in the chemical shift range of 1–2 ppm relative to bulk water. Furthermore, there was no correlation between Eu concentration and CEST effect. These experiments suggest that the observed CEST effect is due to the liposome membrane itself rather than Eu within the liposome cavity. These results are fully consistent with a recent demonstration of a CEST effect using diamagnetic liposomes that contained cholesterol and, of particular importance, the proton signal at ~1 ppm downfield from bulk water was assigned to hydroxyl protons.<sup>27</sup> Additional support for

<sup>†</sup>Electronic supplementary information (ESI) available: Experimental procedures, preparation of hydration solution, preparation of liposomes, raw CEST data, Lorentzian function fitting, and dynamic light scattering data. See DOI: 10.1039/c4cc07027e

our observations can be found in a previous report of magnetization transfer for a lipid and cholesterol system in which magnetization transfer exhibited a strong dependence on cholesterol concentration (30–60 mol%),<sup>29</sup> and the concentration of cholesterol in our system (42 mol%) falls in this range. Furthermore, our data provide an explanation for the observation of CEST before oxidation of  $\text{Eu}^{2+}$  by revealing an exchange between the liposome membrane and bulk water. In this proposed exchange mechanism,  $\text{Eu}(\text{2.2.2})^{2+}$  is confined to the intraliposomal cavity and, consequently, would not interact with protons exchanging on the outer surface of the liposome.

To visualize the nature of the  $\text{Eu}^{2+/3+}$  responses, we acquired *in vitro* images of suspensions of our liposomes before and after air exposure (Fig. 4). The  $T_1$ -weighted images confirmed positive contrast enhancement for the  $\text{Eu}(\text{2.2.2})^{2+}$ -containing liposomes and also revealed no significant difference in signal intensity between water and the oxidized  $\text{Eu}^{3+}$ -containing liposomes at the 95% confidence interval (Student's *t*-test). Consistent with our NMR studies that showed an 86% decrease in  $T_1$  after exposure to air, there was an 81% decrease in signal intensity in  $T_1$ -weighted images before and after oxidation. To quantify the CEST effect, the phantom image intensities were used to calculate %CEST defined as  $(1 - M_z/M_0)100$ , where  $M_z$  and  $M_0$  are the average signal intensities at the on- and off-resonance positions.<sup>30</sup> The CEST map confirmed the presence of exchangeable protons before and after oxidation and that %CEST was not significantly different after oxidation based on the standard error of the CEST effect measurements in Fig. 2. Based on our control experiments, the change in CEST effect is not due to the presence of Eu, despite the influence of  $T_1$  on the CEST effect.<sup>31</sup> Nevertheless, these data demonstrate a distinct dual-mode response and reveal the oxidation state of Eu without knowledge of its concentration. Therefore, (1) if  $T_1$  enhancement and CEST effect are both present, the agent has not responded. Similarly, (2) if  $T_1$  enhancement is no longer observed and CEST effect is still present, then the agent has responded. If neither forms of contrast are detected, then (3) the agent is no longer present or is present at a level below the detection limit of MRI. Based on these three scenarios, one can determine the oxidation state of Eu (and therefore a response) without knowledge of the concentration of Eu. This method does not quantify the amount of oxidant present, but reports on the oxidation itself in a concentration-independent manner by using two orthogonal detection modes (one of which changes and one of which does not change in response to oxidation).

With this demonstration of distinct orthogonal imaging, we envision tracking the migration of the contrast agent with  $T_1$ -weighted imaging. Upon disappearance of  $T_1$  enhancement, the imaging mode of detection would be changed to CEST. The presence of CEST effect would indicate oxidation, and an absence of CEST effect would indicate clearance of the contrast agent. Furthermore, CEST effect could be used to indicate one or more specific disease states because the oxidation potential, and consequently loss of  $T_1$  enhancement, of  $\text{Eu}(\text{2.2.2})^{2+}$  is tunable through ligand structure modifications.<sup>20</sup> Accordingly, our *in vitro* data provide a strong framework for optimizing our system for *in vivo* imaging.

The kinetic stability of  $\text{Eu}(\text{2.2.2})^{3+}$  relative to  $\text{Eu}(\text{2.2.2})^{2+}$  is of importance because of the toxic nature of uncomplexed trivalent lanthanide ions. It has been demonstrated that  $\text{Eu}(\text{2.2.2})^{3+}$  is less kinetically stable relative to  $\text{Eu}(\text{2.2.2})^{2+}$ ,<sup>32</sup> which is primarily due to the

reduction in size of Eu upon oxidation. To demonstrate that our liposomes did not leach Eu, the oxidized liposomes were filtered, and the Eu concentration of the filtrate was measured to be below the detection limit (<66 nM) of inductively coupled plasma optical emission spectroscopy. This result indicates that the liposome traps uncomplexed  $\text{Eu}^{3+}$ , which is likely present as a species coordinated with phosphate from the buffer, phosphate from the phospholipid membrane, or as the free aqua ion.

In conclusion, we have demonstrated the first oxidation-responsive dual-mode contrast agent for MRI based on the redox chemistry of Eu. Contrast enhancement in orthogonal imaging modes allows for the detection of Eu oxidation states without knowledge of contrast agent concentration. Notably, the response of our system is irreversible due to the stability of  $\text{Eu}^{3+}$  with respect to reduction. Irreversible response is potentially advantageous *in vivo* because the contrast agent is in a dynamic environment and can indicate oxidation even if no longer in the oxidizing region. For these reasons, we expect this system to open the door for molecular imaging using the  $\text{Eu}^{2+/3+}$  redox switch, and we are currently exploring the scope of the system to identify physiologically relevant oxidants and the kinetics of intraliposomal  $\text{Eu}^{2+}$  oxidation.

## Supplementary Material

Refer to Web version on PubMed Central for supplementary material.

## Acknowledgments

The authors acknowledge research support from a Schaap Faculty Scholar Award (M.J.A.) and the National Institutes of Health (NIH) grant EB013663 (M.J.A.). Imaging time was supported by NIH grant CA129173 (M.M.A.). We thank Mark D. Pagel and Tian Shi for helpful discussions.

## Notes and references

1. (a) Hermann P, Kotek J, Kubí ek V, Lukeš I. Dalton Trans. 2008:3027. [PubMed: 18521444] (b) Radecki G, Nargeot R, Jelescu IO, Le Bihan D, Ciobanu L. Proc Natl Acad Sci U S A. 2014; 111:8667. [PubMed: 24872449]
2. Wu Y, Soesbe TC, Kiefer GE, Zhao P, Sherry AD. J Am Chem Soc. 2010; 132:14002. [PubMed: 20853833]
3. (a) Torres E, Mainini F, Napolitano R, Fedeli F, Cavalli R, Aime S, Terreno E. J Controlled Release. 2011; 154:196. Opina ACL, Wu Y, Zhao P, Kiefer G, Sherry AD. Contrast Media Mol Imaging. 2011; 6:(b). 459. Ali MM, Woods M, Caravan P, Opina ACL, Spiller M, Fettinger JC, Sherry AD. Chem – Eur J. 2008; 14:(c). 7250. Tóth É, Bolskar RD, Borel A, González G, Helm L, Merbach AE, Sitharaman B, Wilson LJ. J Am Chem Soc. 2005; 127:(d). 799. Woods M, Kiefer GE, Bott S, Castillo-Muzquiz A, Eshelbrenner C, Michaudet L, McMillan K, Mudigunda SDK, Ogrin D, Tircsó G, Zhang S, Zhao P, Sherry AD. J Am Chem Soc. 2004; 126:(e). 9248.
4. (a) Coman D, Kiefer GE, Rothman DL, Sherry AD, Hyder F. NMR Biomed. 2011; 24:1216. [PubMed: 22020775] (b) Langereis S, Keupp J, van Velthoven JLJ, de Roos IHC, Burdinski D, Pikkemaat JA, Grüll H. J Am Chem Soc. 2009; 131:1380. [PubMed: 19173663] (c) Zhang S, Malloy CR, Sherry AD. J Am Chem Soc. 2005; 127:17572. [PubMed: 16351064]
5. (a) Que EL, Gianolio E, Baker SL, Wong AP, Aime S, Chang CJ. J Am Chem Soc. 2009; 131:8527. [PubMed: 19489557] (b) Li W, Fraser SE, Meade TJ. J Am Chem Soc. 1999; 121:1413.(c) Trokowski R, Ren J, Kálmán FK, Sherry AD. Angew Chem, Int Ed. 2005; 44:6920.
6. (a) Hingorani DV, Randtke EA, Pagel MD. J Am Chem Soc. 2013; 135:6396. [PubMed: 23601132] (b) Moats RA, Fraser SE, Meade TJ. Angew Chem, Int Ed Engl. 1997; 36:726.

7. Liu G, Liang Y, Bar-Shir A, Chan K W Y, Galpoththawela CS, Bernard SM, Tse T, Yadav NN, Walczak P, McMahon MT, Bulte JWM, van Zijl PCM, Gilad AA. *J Am Chem Soc.* 2011; 133:16326. [PubMed: 21919523]
8. Aime S, Botta M, Gianolio E, Terreno E. *Angew Chem, Int Ed.* 2000; 39:747.
9. (a) Gløgaard C, Stensrud G, Aime S. *Magn Reson Chem.* 2003; 41:585.(b) Liu G, Li Y, Pagel MD. *Magn Reson Med.* 2007; 58:1249. [PubMed: 18046705]
10. Ratnakar SJ, Soesbe TC, Lumata LL, Do QN, Viswanathan S, Lin CY, Sherry AD, Kovacs Z. *J Am Chem Soc.* 2013; 135:14904. [PubMed: 24050192]
11. Huang CH, Hammell J, Ratnakar SJ, Sherry AD, Morrow JR. *Inorg Chem.* 2010; 49:5963. [PubMed: 20509631]
12. Song B, Wu Y, Yu M, Zhao P, Zhou C, Kiefer GE, Sherry AD. *Dalton Trans.* 2013; 42:8066. [PubMed: 23575743]
13. Loving GS, Mukherjee S, Caravan P. *J Am Chem Soc.* 2013; 135:4620. [PubMed: 23510406]
14. Tsitovich PB, Sperryak JA, Morrow JR. *Angew Chem.* 2013; 125:14247.
15. (a) Facciabene A, Peng X, Hagemann IS, Balint K, Barchetti A, Wang LP, Gimotty PA, Gilks CB, Lal P, Zhang L, Coukos G. *Nature.* 2011; 475:226. [PubMed: 21753853] (b) Shweiki D, Itin A, Soffer D, Keshet E. *Nature.* 1992; 359:843. [PubMed: 1279431]
16. Karhausen J, Furuta GT, Tomaszewski JE, Johnson RS, Colgan SP, Haase VH. *J Clin Invest.* 2004; 114:1098. [PubMed: 15489957]
17. Weir EK, López-Barneo J, Buckler KJ, Archer SL. *N Engl J Med.* 2005; 353:2042. [PubMed: 16282179]
18. Aime S, Fedeli F, Sanino A, Terreno E. *J Am Chem Soc.* 2006; 128:11326. [PubMed: 16939235]
19. Terreno E, Boffa C, Menchise V, Fedeli F, Carrera C, Castelli DD, Digilio G, Aime S. *Chem Commun.* 2011; 47:4667.
20. Gamage NDH, Mei Y, Garcia J, Allen MJ. *Angew Chem, Int Ed.* 2010; 49:8923.
21. (a) Garcia J, Neelavalli J, Haacke EM, Allen MJ. *Chem Commun.* 2011; 47:12858.(b) Garcia J, Kuda-Wedagedara ANW, Allen MJ. *Eur J Inorg Chem.* 2012:2135. [PubMed: 22639543]
22. Burai L, Scopelliti R, Tóth E. *Chem Commun.* 2002:2366.
23. (a) Aime S, Castelli DD, Terreno E. *Angew Chem, Int Ed.* 2005; 44:5513.(b) Zhao JM, Har-el Y, McMahon MT, Zhou J, Sherry AD, Sgouros G, Bulte JWM, van Zijl PCM. *J Am Chem Soc.* 2008; 130:5178. [PubMed: 18361490]
24. Gianolio E, Porto S, Napolitano R, Baroni S, Giovanzana GB, Aime S. *Inorg Chem.* 2012; 51:7210. [PubMed: 22716284]
25. (a) Moats RA, Fraser SE, Meade TJ. *Angew Chem, Int Ed Engl.* 1997; 36:726.(b) Duimstra JA, Femia FJ, Meade TJ. *J Am Chem Soc.* 2005; 127:12847. [PubMed: 16159278] (c) Hanaoka K, Kikuchi K, Urano Y, Nagano T. *J Chem Soc, Perkin Trans 2.* 2001:1840.(d) Hanaoka K, Kikuchi K, Urano Y, Narazaki M, Yokawa T, Sakamoto S, Yamaguchi K, Nagano T. *Chem Biol.* 2002; 9:1027. [PubMed: 12323377] (e) Hifumi H, Tanimoto A, Citterio D, Komatsu H, Suzuki K. *Analyst.* 2007; 132:1153. [PubMed: 17955150] (f) Tu C, Osborne EA, Louie AY. *Tetrahedron.* 2009; 65:1241. [PubMed: 20126289] (g) Martinelli J, Fekete M, Tei L, Botta M. *Chem Commun.* 2011; 47:3144.(h) Shuhendler AJ, Staruch R, Oakden W, Gordijo CR, Rauth AM, Stanisz GJ, Chopra R, Wu XY. *J Controlled Release.* 2012; 157:478.(i) Xu W, Lu Y. *Chem Commun.* 2011; 47:4998.(j) Catanzaro V, Gringeri CV, Menchise V, Padovan S, Boffa C, Dastrù W, Chaabane L, Digilio G, Aime S. *Angew Chem, Int Ed.* 2013; 52:3926.
26. Aime S, Castelli DD, Lawson D, Terreno E. *J Am Chem Soc.* 2007; 129:2430. [PubMed: 17288421]
27. Liu G, Moake M, Har-el Y, Long CM, Chan K W Y, Cardona A, Jamil M, Walczak P, Gilad AA, Sgouros G, van Zijl PCM, Bulte JWM, McMahon MT. *Magn Reson Med.* 2012; 67:1106. [PubMed: 22392814]
28. (a) Longo DL, Dastrù W, Digilio G, Keupp J, Langereis S, Lanzardo S, Prestigio S, Steinbach O, Terreno E, Uggeri F, Aime S. *Magn Reson Med.* 2011; 65:202. [PubMed: 20949634] (b) Zheng S, van der Bom IMJ, Zu Z, Lin G, Zhao Y, Gounis MJ. *Magn Reson Med.* 2014; 71:1082. [PubMed: 23661508] (c) Chan K W Y, Yu T, Qiao Y, Liu Q, Yang M, Patel H, Liu G, Kinzler KW, Vogelstein B, Bulte JWM, van Zijl PCM, Hanes J, Zhou S, McMahon MT. *J Controlled Release.*



- 2014; 180:51.(d) Sun PZ, Wang E, Cheung JS, Zhang X, Benner T, Sorensen AG. *Magn Reson Med.* 2011; 66:1042. [PubMed: 21437977] (e) Bar-Shir A, Liu G, Liang Y, Yadav NN, McMahon MT, Walczak P, Nimmagadda S, Pomper MG, Tallman KA, Greenberg MM, van Zijl PCM, Bulte JWM, Gilad AA. *J Am Chem Soc.* 2013; 135:1617. [PubMed: 23289583]
29. Fralix TA, Ceckler TL, Wolff SD, Simon SA, Balaban RS. *Magn Reson Med.* 1991; 18:214. [PubMed: 2062233]
30. Opina ACL, Ghaghada KB, Zhao P, Kiefer G, Annapragada A, Sherry AD. *PLoS One.* 2011; 6:e27370. [PubMed: 22140438]
31. van Zijl PCM, Yadav NN. *Magn Reson Med.* 2011; 65:927. [PubMed: 21337419]
32. Yee EL, Gansow OA, Weaver MJ. *J Am Chem Soc.* 1980; 102:2278.

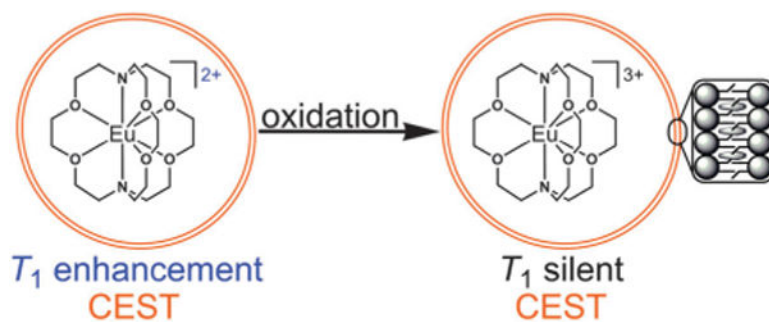


**Fig. 1.** Representation of the oxidation of liposome-encapsulated  $\text{Eu}(2.2.2)^{2+}$  ( $T_1$  enhancement and CEST effect) to form a liposome filled with  $\text{Eu}^{3+}$  ( $T_1$  silent with CEST effect). On the far right is a depiction of the liposomal phospholipid bilayer with ovals as cholesterol molecules. For clarity, only one complex is shown in each liposome and coordinated water molecules are not drawn.



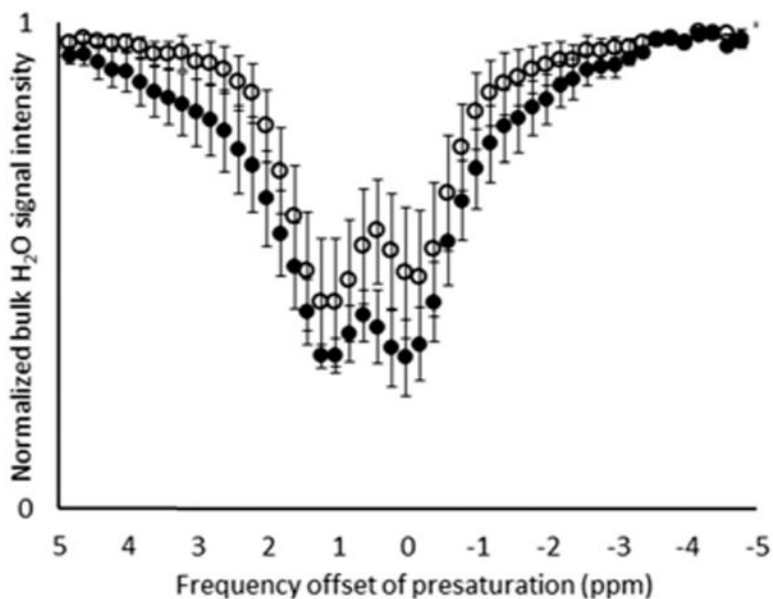


**Fig. 2.** CEST spectra (7 T and 24 °C) of Eu(2.2.2)<sup>2+</sup>-containing liposomes before (○) and after (●) 24 h air exposure. Data points represent the mean of six independently prepared samples [liposomes containing only phosphate-buffered saline; Sr(2.2.2)<sup>2+</sup> (28 mM Sr); and Eu(2.2.2)<sup>2+</sup> (13, 24, 40, and 45 mM Eu)], and error bars represent the standard error of the mean. The upfield signal was referenced to 0 ppm using the Lorentzian-fitted spectra and signal intensities were calculated from *in vitro* images after a 2 s presaturation with a 17 μT radiofrequency pulse from 5 to -5 ppm in 0.2 ppm increments.

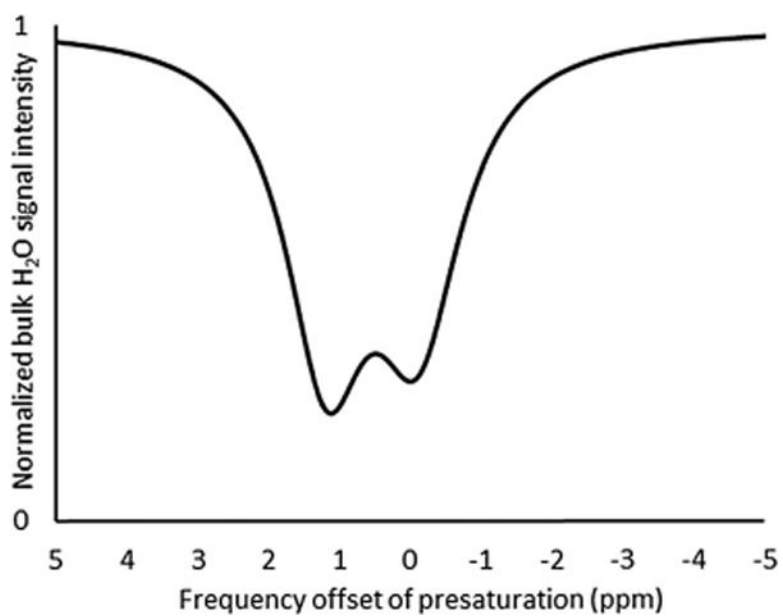


**Fig. 3.** Lorentzian-fitted CEST spectrum (7 T and 24 °C) of liposomes filled with phosphate-buffered saline. The upfield signal was referenced to 0 ppm, and signal intensities were calculated from *in vitro* images after a 2 s presaturation with a 17  $\mu$ T radiofrequency pulse from 5 to -5 ppm in 0.2 ppm increments.

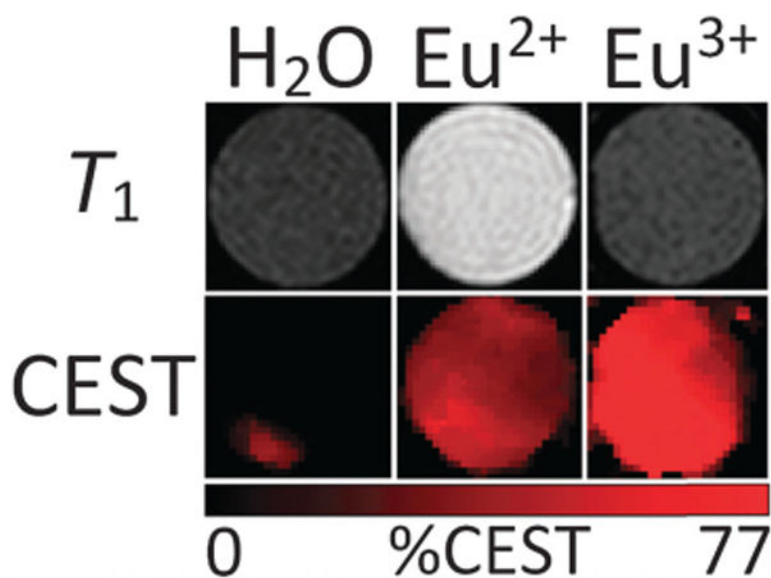


**Fig. 4.** MR phantom images (5 mm tube diameter) at 7 T and 24 °C of water, non-oxidized liposomes containing Eu<sup>2+</sup>, and oxidized liposomes containing Eu<sup>3+</sup>. In the top row are T<sub>1</sub>-weighted images and on the bottom is a CEST map generated by subtracting presaturation at 1.2 ppm from presaturation at -1.2 ppm and the difference was divided by presaturation at -1.2 ppm. %CEST represents the decrease in bulk water signal intensity as a result of presaturation exchangeable water protons associated with liposomes. Based on the error associated with the CEST imaging, the difference between the Eu<sup>2+</sup> and Eu<sup>3+</sup> samples is not significant.